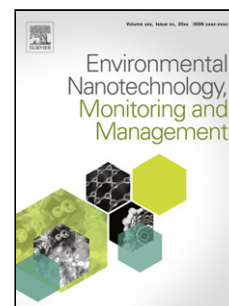


Journal Pre-proof

BENTONITE-COMPOSITE POLYVINYL ALCOHOL/ALGINATE HYDROGEL BEADS: PREPARATION, CHARACTERIZATION AND THEIR USE AS ARSENIC REMOVAL DEVICES

Estefanía Baigorria (Conceptualization) (Methodology) (Validation) (Investigation) (Writing - original draft) (Writing - review and editing) (Supervision), Leonardo A. Cano (Conceptualization) (Methodology) (Validation) (Investigation) (Writing - original draft) (Writing - review and editing) (Supervision), Laura M. Sanchez (Conceptualization) (Methodology) (Validation) (Investigation) (Writing - original draft) (Writing - review and editing) (Supervision) (Project administration), Vera A. Alvarez (Conceptualization) (Writing - original draft) (Writing - review and editing) (Supervision) (Resources) (Project administration) (Funding acquisition), Romina P. Ollier (Conceptualization) (Methodology) (Validation) (Investigation) (Writing - original draft) (Writing - review and editing) (Supervision) (Resources) (Project administration) (Funding acquisition)



PII: S2215-1532(20)30346-9
DOI: <https://doi.org/10.1016/j.enmm.2020.100364>
Reference: ENMM 100364

To appear in: *Environmental Nanotechnology, Monitoring & Management*

Received Date: 21 April 2020
Revised Date: 14 June 2020
Accepted Date: 25 August 2020

Please cite this article as: Baigorria E, Cano LA, Sanchez LM, Alvarez VA, Ollier RP, BENTONITE-COMPOSITE POLYVINYL ALCOHOL/ALGINATE HYDROGEL BEADS: PREPARATION, CHARACTERIZATION AND THEIR USE AS ARSENIC REMOVAL DEVICES, *Environmental Nanotechnology, Monitoring and amp; Management* (2020),

doi: <https://doi.org/10.1016/j.enmm.2020.100364>

This is a PDF file of an article that has undergone enhancements after acceptance, such as the addition of a cover page and metadata, and formatting for readability, but it is not yet the definitive version of record. This version will undergo additional copyediting, typesetting and review before it is published in its final form, but we are providing this version to give early visibility of the article. Please note that, during the production process, errors may be discovered which could affect the content, and all legal disclaimers that apply to the journal pertain.

© 2020 Published by Elsevier.

BENTONITE-COMPOSITE POLYVINYL ALCOHOL/ALGINATE HYDROGEL BEADS: PREPARATION, CHARACTERIZATION AND THEIR USE AS ARSENIC REMOVAL DEVICES.

Estefanía Baigorria, Leonardo A. Cano, Laura M. Sanchez, Vera A. Alvarez and Romina P. Ollier*

Materiales Compuestos Termoplásticos (CoMP), Instituto de Investigaciones en Ciencia y Tecnología de Materiales (INTEMA), CONICET - Universidad Nacional de Mar del Plata (UNMDP). Av. Colón 10890, Mar del Plata, 7600, Argentina.

*Corresponding author: Dr. Romina P. Ollier. Phone N°: (+54 223) 62606270; e-mail:

*rominaollier@fi.mdp.edu.ar

Graphical abstract



Highlights

- Composite hydrogel beads based on PVA, sodium alginate and bentonite were prepared by ionic gelation.
- The resulting beads were tested for arsenic removal from waste water.
- Wet beads were highly porous and spherical.
- The incorporation of bentonite produced a reduction on the swelling degree and an increase of gel fraction of the beads.
- The clay inclusion plays a key role in the As removal.

Abstract

Arsenic (As) is a major source of water contamination that has both natural and anthropogenic origins, so that, to remove it from water is a relevant topic. Taking into account the ease of operation, the cost of processing and the required instrumentation, adsorption processes could be considered as very convenient alternative technologies for water remediation. The present research work is focused on the development and characterization of eco-friendly polyvinyl alcohol (PVA) and alginate (Alg) hydrogel beads containing natural bentonite (Bent) as potential useful devices for As removal from polluted water. Composite beads with different PVA/Alg proportions (75/25 and 50/50) with and without 30 wt.% Bent were prepared by ionic gelation. The obtained beads were thoroughly characterized by means of thermal analysis (differential scanning calorimetry and thermogravimetric analysis), crosslinking degree by evaluating the gel fraction (GF), the capacity of swelling, morphological aspects (by Scanning Electron Microscopy), functional groups and interactions (by FTIR) and finally, the performance of the beads as arsenic adsorbent was tested by treating batch aqueous solutions. Morphological investigations showed that wet beads were highly porous and spherical. Moreover, the beads with the highest PVA content absorbed higher amounts of water whereas the incorporation of clay to the hydrogels produced a reduction on the swelling degree and an increase of GF. The adsorption behavior of the pearls towards As was studied in terms of PVA/Alg ratio, clay loading and contact time. The results clearly demonstrated that the clay inclusion plays a key role in the As removal since unfilled PVA/Alg beads were not able to remove it. The FTIR spectra of beads after As removal show the partial migration of the components of the beads, which can be associated with the intermediate crosslinking degree and almost amorphous state within the matrix.

Keywords: Bentonite, Polyvinyl Alcohol, Sodium Alginate, Hydrogel; Arsenic, Environmental Remediation.

1. Introduction

The need for having water resources of appropriate quality is a topic of worldwide concern. Due to a very broad set of reasons water bodies are polluted thus affecting nature, and seriously compromising the future health of living organisms. In particular, Arsenic (As) is a major source of water contamination that has both natural and anthropogenic origins, and it exists in different oxidation states depending on the pH of the environment (Rahim and Mas Haris, 2015; Safi et al., 2019). Many countries are facing As contaminated groundwater problems, such as Argentina, Bangladesh, Chile, China, India, Japan, Mexico, Mongolia, Nepal, Philippines, Poland, Taiwan, Thailand and Vietnam, among some other ones (Peralta Ramos et al., 2016; Tajuddin Sikder et al., 2014). The exposure to As could lead to have injuries to central nervous system, diseases of respiratory, peripheral vascular, cardiovascular and cerebrovascular systems, diabetes mellitus, hypertension and carcinogenic diseases (urinary tract, liver, skin, kidneys, large intestine, buccal cavity, bone, lungs and rectum cancers) (Guan et al., 2012; Rahim and Mas Haris, 2015; Safi et al., 2019; Thomas et al., 2001). Since drinking water could be considered as the main exposure source to arsenic, achieve its successful removal is a mandatory need (Dopp et al., 2010; Guo et al., 2015).

There are a lot of options regarding water bodies remediation treatments. Their most wide classification considers chemical, physical and biological procedures. (Lodha and Chaudhari, 2007; Ratna, D., Padhi, 2012; Slokar and Majcen Le Marechal, 1998), (Al-Bastaki, 2004; Golob et al., 2005; Ratna, D., Padhi, 2012). (Ratna, D., Padhi, 2012; Robinson et al., 2001). Taking into account the ease of operation, the cost of processing and the required instrumentation, adsorption processes could be considered as very convenient alternative technologies for water remediation (Khurana et al., 2017; Paulino et al., 2011; Sanchez, L. M., Ollier, R. P., Gonzalez, J. S., Alvarez, 2018).

Clays are low cost, abundant natural occurring negatively charged aluminosilicates. Various studies have revealed that both natural and modified clays have good to excellent performances for toxic heavy metals and concisely As adsorption in water treatments (García-Carvajal, C., Villarroel-Rocha, J., Curvale, D., Barroso-Quiroga, M. M., Sapag, 2019; Hua, 2015).

Specifically, the application of bentonite as an adsorbent is related mainly to its high cation exchange capacity, large surface area and ease of chemical functionalization (Hua, 2015). Even though the specific arsenic adsorption mechanism on clays is still under discussion, two main phenomena might be considered as the most probably intervening ones: the formation of strong superficial complexes with octahedrally-coordinated aluminum; and the sorption on positively charged Al and Fe hydroxides that are usually found as clay particles coatings (Ghorbanzadeh et al., 2015; Goldberg, 2002; Halter and Pfeifer, 2001; Mohapatra et al., 2007). Nevertheless, most of the authors agree that clays should be immobilized in a suitable polymer matrix to facilitate handling and possibly be reused easier (Perez et al., 2020; Laura M Sanchez et al., 2019; Laura M. Sanchez et al., 2019; Sanchez et al., 2020).

Hydrogels are widely being considered and used as adsorbents since they not only have a high swelling and adsorption capability but also can be easily manipulated, regenerated and reused (Pathan and Bose, 2018). In short, hydrogels are physically or chemically crosslinked three-dimensional networks whose probably most outstanding characteristic is related to their large swelling capability (Bera, R., Dey, A., Chakrabarty, 2015; Kushwaha et al., 2012; Masteiková, R., Chalupová, Z., Sklupalová, 2013; Qiu and Park, 2001; Ramteke, n.d.). The hydrogels adsorption capacity could be tuned to have selective removal towards a desired pollutant by properly designing the materials during the preparation process. For example, functional groups with certain charges could be introduced by selecting the starting materials useful as hydrogel matrix (Khan and Lo, 2016; Mahdavinia et al., 2018; Ozay et al., 2009); and the general morphology and pores sizes could also be conveniently controlled not only by the employment of chemical substances but also by using specific preparation protocols (Dinu et al., 2013; Sanchez, L. M., Alvarez, 2019). Furthermore, the incorporation of fillers may lead to have composite hydrogels that in most cases offer unique properties. In this sense, sorption, thermal, chemical and mechanical properties have been modified by adding small amounts of different inorganic nanometric fillers, such as carbon, clays, metal and metal oxides (Sanchez, L. M.,

Ollier, R. P., Gonzalez, J. S., Alvarez, 2018; Sinha Ray and Okamoto, 2003; Sun, Y., Zhang, Z., Moon, K. S., Wong, 2004).

Recently, the use of natural polymers for the design of eco-friendly nanocomposite adsorbents has been the subject of great interest. Several biobased hydrogel devices were tested as adsorbents for As removal from polluted water, such as chitin-, chitosan- and sodium alginate-based ones (Pathan and Bose, 2018; Peralta Ramos et al., 2016; Safi et al., 2019; Sahiner et al., 2011). Sodium alginate (Alg) is a non-toxic, biodegradable copolymer polysaccharide, which is composed of linearly (1–4)-linked β -D-mannuronic acid and α -L-guluronic acid. This widely available polymer can be extracted from brown algae (Paques et al., 2014). Ionotropic gelation with divalent metal ions, such as Ca^{+2} , is an easy and effective method to crosslink Alg for the fabrication of spherical hydrogel beads (Hua et al., 2010). The blending of Alg with other polymers such as polyvinylalcohol (PVA) has been proposed in order to overcome the quick breakdown of hydrated Ca-Alg beads. PVA is a polyhydroxylated, biocompatible polymer that has been widely used for hydrogels preparation due to its hydrophilic and ease-to processing characteristics (Peppas and Tennenhouse, 2004). In addition, PVA can be physically crosslinked through the formation of crystallites by freezing thawing cycles (Hassan and Peppas, 2000; Lozinsky and Plieva, 1998).

In light of these facts, in the present study it is reported as a novelty, the preparation and characterization of composite macroporous hydrogel beads as potential As removal devices, based on eco-friendly and economic raw materials (Alg, PVA and Bent) and processing technique (Ca^{+2} crosslinking). To the best of our knowledge, there is no previous research work conducted by employing these starting materials combination to generate bead devices for the use here proposed.

2. Materials and methods

2.1. Materials

PVA with molecular weight of 31000-51000 g/mol and hydrolysis degree of 98-99% was supplied by Sigma-Aldrich. Alg was purchased to Química Bolívar, whereas the clay employed in this work was a bentonite (Bent) supplied by Minarmco S.A. (Neuquén, Argentina). The raw clay consisted predominantly of montmorillonite, as detailed in a previous work (D'Amico et al., 2014). The basal spacing was 1.3 nm and its cation exchange capacity was found to be 0.939 meq g⁻¹, and the content of Fe (III) is 27.3%. Chlorhydric acid (HCl; 36.5–38%) and ammonium hydroxide (NH₄OH; 25–30%) were supplied by Ciccarelli (San Lorenzo, Argentina); whereas calcium chloride (CaCl₂), arsenic oxide (As₂O₃), and methyl orange dye (MO) were all supplied by Biopack (Buenos Aires, Argentina). Hydrazine sulfate (NH₂NH₂·H₂SO₄), potassium bromate (KBrO₃) and ammonium molybdate ((NH₄)₆Mo₇O₂₄·4H₂O) were acquired from Anedra (Buenos Aires, Argentina).

2.2. Methods

2.2.1. Beads preparation

An aqueous solution containing PVA and Alg was prepared by heating at 85°C during 4 h under constant magnetic stirring. Two formulations were prepared all of them reaching a final polymeric concentration of 1.0 g/ 15 mL: 0.5 g PVA/ 0.5 g Alg and 0.75 g PVA/ 0.25 g Alg. Then, 0.3 g of Bent were added, and the suspension was vigorously stirred in a vortex during 1 min. The as obtained suspension was added dropwise into 100 mL of a CaCl₂ solution (0.3 M) keeping constant magnetic stirring during 30 min at room temperature. Spherical, smooth and homogenous beads were thus obtained and were subsequently washed three times with distilled water. Blank PVA/Alg samples of each considered formulation were also prepared by following the same general procedure, but without the addition of the clay.

2.2.2. Beads characterization

Thermogravimetric analysis (TGA) was performed in TA-Q500 equipment from room temperature to 800 °C at a heating rate of 10 °C min⁻¹ under nitrogen atmosphere, in order to avoid the thermo-oxidative oxidation. Each specimen mass was in the range of 7–15 mg.

Differential scanning calorimetric (DSC) measurements of the dried hydrogels were carried out in TA-Q2000 DSC equipment, under N₂ atmosphere. Each sample was heated from room temperature to 40 °C, maintained isothermally for 10 min, cooled to -20 °C, heated from -20 to 255 °C at 5 °C min⁻¹, and then cooled again. The crystallinity degree (Xcr%) was calculated from the following equation (Eq. 1):

$$X_{cr} (\%) = \frac{\Delta H}{\Delta H^0 \times W_{PVA}} \quad (\text{Equation 1})$$

where ΔH was determined by integrating the area under the melting peak and ΔH^0 is the heat (138.6 J g⁻¹) required for melting a 100% crystalline PVA sample, whereas W_{PVA} is the mass fraction of the PVA matrix in the hydrogel sample (Peppas, N. A., Hansen, 1982).

Fourier Transformed Infrared Spectroscopy (FTIR) measurements were done employing a resolution of 4 cm⁻¹ in a Thermo Scientific Nicolet 6700 spectrometer. Measurements were carried out from 400 to 4000 cm⁻¹ in attenuated total reflectance modes (smart Orbit ATR accessory).

Gel fraction determinations (GF %) were carried out at 25 °C in distilled water. To perform GF % measurements, samples were immersed into distilled water at room temperature during 4 days. Then, the samples were removed from distilled water and dried until constant weight was reached. Therefore, the gel fraction of each sample was calculated as follows (Eq. 2):

$$GF (\%) = \frac{W_f - W_r}{W_i - W_r} \times 100 \quad (\text{Equation 2})$$

where W_i and W_f are the weights of the dried hydrogels before and after immersion, respectively, and W_r is the weight of the filler added (experimentally determined by TGA).

Swelling degree measurements at 25 °C in distilled water were conducted. The swelling degree (W_t %) at t time was determined by the following equation (Eq. 3):

$$W_t (\%) = \frac{W_f - W_i}{W_i} \times 100 \quad (\text{Equation 3})$$

where W_i is the weight of the samples before immersion and W_f is the weight of the sample at equilibrium water content.

The morphology of the beads was examined by Scanning Electron Micrographs (SEM) in a JEOL JSM-6460 LV instrument. Samples have been previously swollen, frozen, lyophilized, cryofractured with liquid N_2 and sputtered with gold.

2.2.3. Beads performance as arsenic adsorbents

In order to determine the capability of the selected beads towards arsenic adsorption, batch aqueous solutions were treated. The arsenic (III, As) solution concentration was 1 ppm, and the adsorbent/solution ratio was 0.01 g/ 1 mL. The water treatments were applied at room temperature during different periods being the longest considered of 48 h. All tests were run on duplicate. The removal efficiency was determined by measuring the remaining As in the water samples through the already well-known molybdene blue colorimetric method (Lenoble et al., 2003) by using a SQ- 2800E UNICO diode array UV-Visible spectrometer. The method determines the As (V) concentration and the detection limited is 0.02 ppm of As (V) (Lenoble et al., 2003). The obtained results are expressed as Removal efficiency (R_t) at t time (Equation 4):

$$R_t (\%) = \frac{C_0 - C_t}{C_0} \times 100 \quad (\text{Equation 4})$$

where C_0 (mg/L) refers to the initial concentration of the As solution, and C_t (mg/L) corresponds to the remaining concentration at t time.

3. Results and Discussion

3.1. Morphological characterization

It could be seen that the swollen beads were spherical with an approximate diameter between 4 and 5 mm. It is important to note that in dry state, after drying in the air or in an oven at 40 °C, their diameter was considerably reduced to about 1.5 mm and when rehydrating the initial size was not recovered so it could be inferred that a partial collapse of the polymer network occurs during the evaporation process of water in the drying process. Therefore, it was decided to keep them in the wet state and to perform the analyzes, the samples were previously freeze-dried and lyophilized.

Figure 1 shows SEM micrographs of the beads and their cross sections for both systems with and without Bent. In all cases it can be seen that materials with compact surface and a robust and well defined porous internal structure were obtained. In the case of unfilled PVA / Alg beads, large pores with smooth walls can be noticed. Larger and higher porosity pearls were obtained when the Alg content is higher, which is consistent with the literature (Ghasemzadeh and Ghanaat, 2014). The incorporation of Bent produced a clear decrease in the size of the pores and in the thickness of its walls. It is also possible to notice an increase in the roughness of the walls of the pores, this fact has already been reported by our research group (Gonzalez, J. S., Ponce, A., Alvarez, 2016; Ollier, R. P., Sanchez, L. M., Gonzalez, J. S., Alvarez, 2018; Laura M. Sanchez et al., 2019). On the other hand, there was a slight increase in the size of the beads compared to the unfilled systems. It can be observed that the clay is homogeneously distributed in the polymer matrix without the presence of macroscopic aggregates. This fact along with the roughness of the pore walls, provide more contact sites which may contribute to a better As sorption.

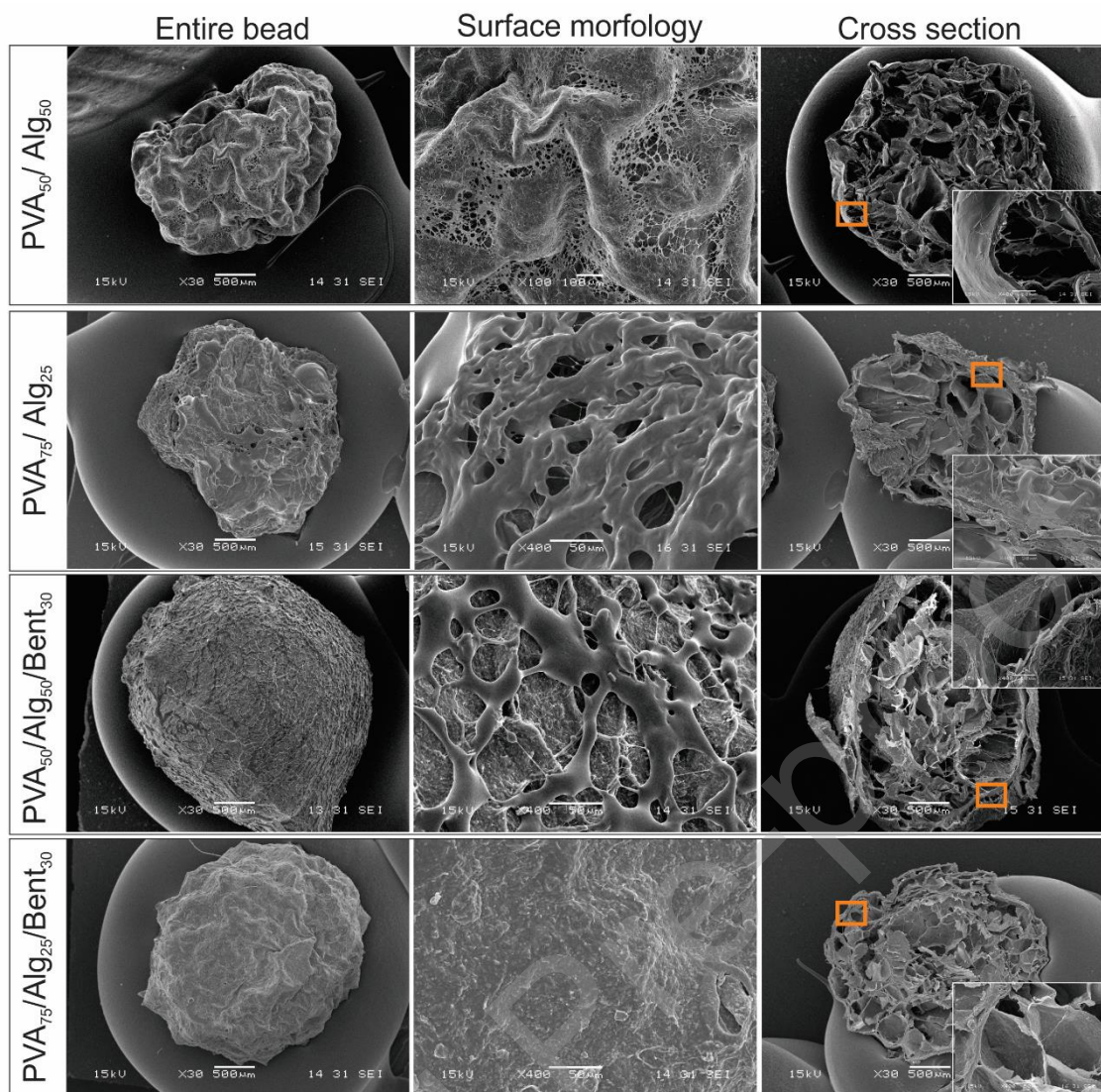


Figure 1. SEM micrographs of the beads.

3.1. Thermal characterizations

Figure 2 shows the TGA and DTGA curves of the beads with and without Bent; they show the loss of characteristic mass of the different components thereof. The thermal degradation of PVA occurs in three stages: the first one is correlated with the evaporation of physisorbed water, between 100 and 180 °C; the second one (between 200 and 300 °C) is attributed to the PVA elimination reactions (a lateral peak accompanies the main peak); while the third stage (425–440 °C) is attributed to PVA chain cleavage reactions (Ollier, R. P., Sanchez, L. M., Gonzalez, J. S., Alvarez, 2018). Alg is also thermally degraded in three stages: the first one is related to dehydration (100–200 °C), the second stage as to the decomposition of the main chain (200–585

°C) and the third stage is due to the formation of sodium bicarbonate (588–751 °C), leaving residues of carbonized material (Soares et al., 2004). On the other hand, Bent does not show any degradation, and only both processes the loss of physisorbed water near 100 °C and the dehydroxylation that occurs around 600 °C, are evident. In the first and second stages of weight loss, the behavior of the samples is very similar but in the third stage the range of weight loss was shifted to higher temperature values in the cases of hydrogel beads with Bent. These observations are indicative of the improved thermal stability of the hydrogel nanocomposite due to the presence of the clay as previously reported with similar systems (Laura M. Sanchez et al., 2019; Tong et al., 2019). In addition, it is important to note that the incorporation of Bent in the beads produced an increase in the residual mass of the sample compared to the PVA / Alg beads, from 32.9% in PVA₅₀/Alg₅₀ to 51.7% in PVA₅₀/Alg₅₀/Bent₃₀ and from 37,55% in PVA₇₅/Alg₂₅ to 48,8% PVA₇₅/Alg₂₅/Bent₃₀.

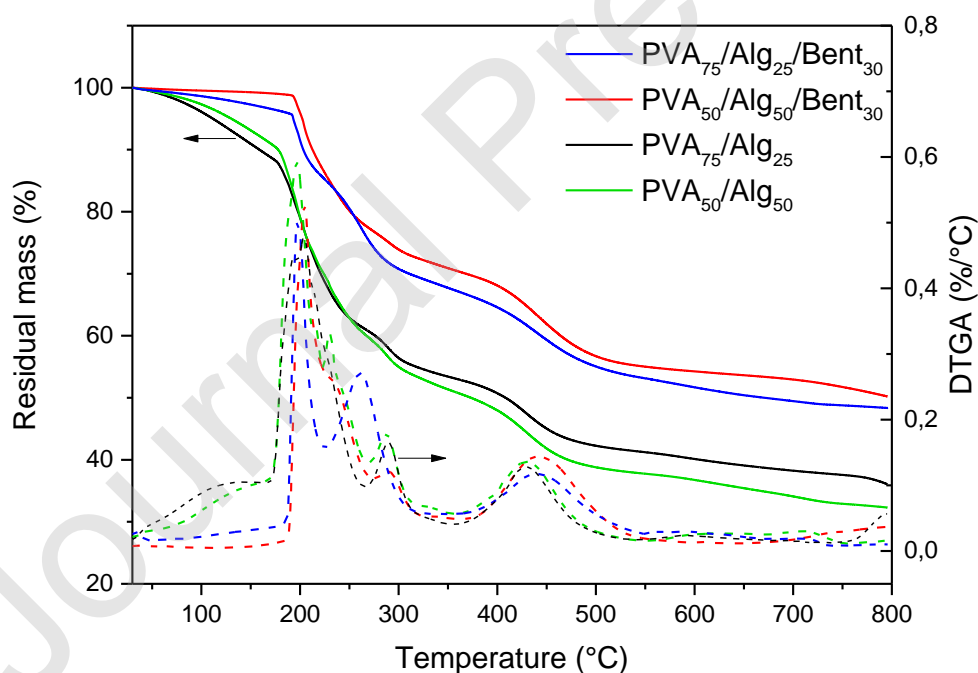


Figure 2. TGA and DTGA thermograms of the samples.

DSC thermograms are shown in **Figure 3** and **Table 1** summarizes glass transition temperature (T_g), the melting temperature (T_m) and crystallinity degree (X_{cr}) values for each sample. A single T_g value is clearly observed in all cases and this suggests that the blends of PVA and Alg are miscible for the two compositions tested and the presence of Bent did not alter this behavior. The increase in the proportion of Alg in the spheres produces an increase in the value of T_g . Some authors attribute this behavior to the hydrogen bonding interactions between PVA and Alg units of these blends (Çaykara and Demirci, 2006). Apparently, the mobility of the chains decreases due to the presence of hydrogen bonds that acts as physical crosslinks. An exothermic peak is evidenced at 190-200 °C and it can be attributed to the decomposition of sodium alginate (Santagapita et al., 2012; Soares et al., 2004), whereas in the case of beads with Bent there is an evident shift of this temperature to higher values. A second endothermic event was observed after this exothermic peak corresponding to PVA melting and all values were found within the typical temperature range for crystalline domains of PVA (Laura M. Sanchez et al., 2019). Apparently, the presence of Bent slightly stabilizes this melting peak in the case of both studied systems, which may possibly be as a result of hydrogen bonding interactions between the clay platelets and PVA chains. It also can be seen that the values obtained for X_{cr} are extremely low for all the cases, indicating that the PVA is at an amorphous form inside the spheres with walls of Alg that is crosslinked and giving support to the structure. Possibly, the increase of Alg proportion produces a decrease in the capacity of the PVA molecules to form inter-and intramolecular hydrogen bonds (Dutra et al., 2017).

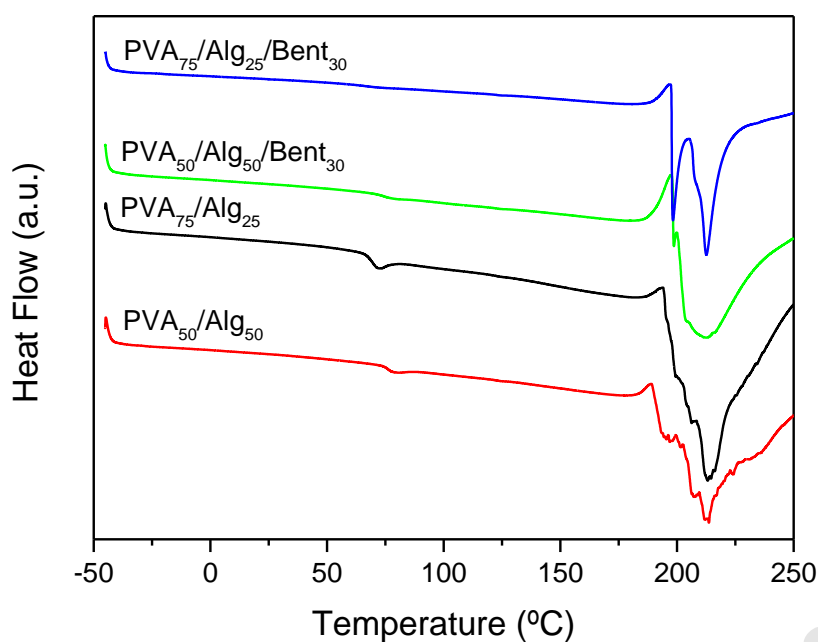


Figure 3. DSC thermograms of the samples.

Table 1. Gel fraction and thermal properties of analyzed beads extracted from DSC analysis.

Sample	T_g (°C)	T_m (°C)	Xcr (%)	GF (%)
PVA ₇₅ /Alg ₂₅	69.6	213.1	2.2	67.9 ± 1.8
PVA ₅₀ /Alg ₅₀	76.1	213.6	2.7	53.8 ± 3.9
PVA ₇₅ /Alg ₂₅ /Bent ₃₀	65.4	198 (1)	0.9 (1)	74.7 ± 1.9
		212 (2)	1.2 (2)	
PVA ₅₀ /Alg ₅₀ /Bent ₃₀	74.3	207.9	3.2	63.5 ± 2.6

3.2. Gel fraction and swelling capability

The swelling degree of the materials as a function of time is plotted in **Figure 4**. As can be seen, the unfilled beads, presented the greater water uptake capabilities. Furthermore, it can be noted that the beads having the highest PVA contents were those that could retain major quantities

of water. Authors have previously observed that composite hydrogels prepared from PVA and modified clays have reduced swelling degree capabilities regarding the neat PVA matrix (Laura M. Sanchez et al., 2019). It is important to remark that the here considered property is strongly dependent on network hydrogel characteristics, as well as gel fraction and pore size (Gonzalez, J. S., Ponce, A., Alvarez, 2016; Kokabi et al., 2007).

Another relevant parameter that should be analyzed is GF which is tabulated in **Table 1**. It can be clearly noticed that GF decreased as the Alg content in the hydrogel beads increased, both in the filled and unfilled systems. Bearing in mind this behavior, it is important to analyze how the beads were obtained. For the preparation of gel beads from Alg solutions by both internal and external ionic gelation methods it is necessary to take into account several considerations, such as the sodium alginate concentration, the bivalent ion-containing solution concentration (such as calcium chloride, for example), the stoichiometric ratio between the starting materials, the temperature and stirring rate established in the reactor, among many others. In the external ionic gelation method, it could be considered that once the sodium alginate droplet contacts the calcium chloride solution almost instantaneously a calcium alginate shell is formed allowing the retention of the shape the original solution had. Thus, at the beginning of gelation process the droplet center is mainly composed of unreacted sodium alginate, which is gradually being turned to calcium alginate when calcium ions penetrate the porous gelled external layer (Kim, 1990). This calcium ions diffusion is a very complex process that has been deeply studied and mathematically modeled by several researchers (Inoue, 1997; Kim, 1990). This considered diffusion process is usually influenced by a number of variables, and even more in the beads that are being presented in this research since the starting Alg solution also contained PVA and, in some cases, Bent. The Alg-Alg, Alg-PVA, Alg-Bent and Alg-Solvent interactions and the corresponding initial Alg-containing solution viscosity of each system should also be considered.

In general, both the gel formation rate and the final morphological characteristics of the prepared beads are influenced by the interaction between calcium ions and Alg. Recently, Rajmohan and Bellmer reported that independently on the gelation methodology, when alginate

concentration increases the shell beads hardness also does it (Rajmohan and Bellmer, 2019). Then, it was also observed that when the shell becomes more rigid, the calcium ions are less favored to entry in the bead during the permanency time already fixed for its crosslinking (Lupo et al., 2015). As a result, when the starting Alg solution concentration is high the corresponding developed bead has a highly crosslinked shell containing a poorly crosslinked core (Lupo et al., 2015), which could lead to observe a decrease in the gel fraction parameter. In accordance to the observations reported by Lupo and coworkers, the beads having the stronger shells are those having an internal structure with larger pores (Lupo et al., 2015).

In addition, the GF value increases when Bent is incorporated into the polymer matrix for both PVA/Alg proportions. This could be attributed to possible interactions between clay and polymer chains through the formation of hydrogen bonds that lead to a hydrogel network with higher crosslinking degree. A similar trend has been reported in literature (Dinu et al., 2017; Laura M. Sanchez et al., 2019), This fact will be discussed later in the FTIR results.

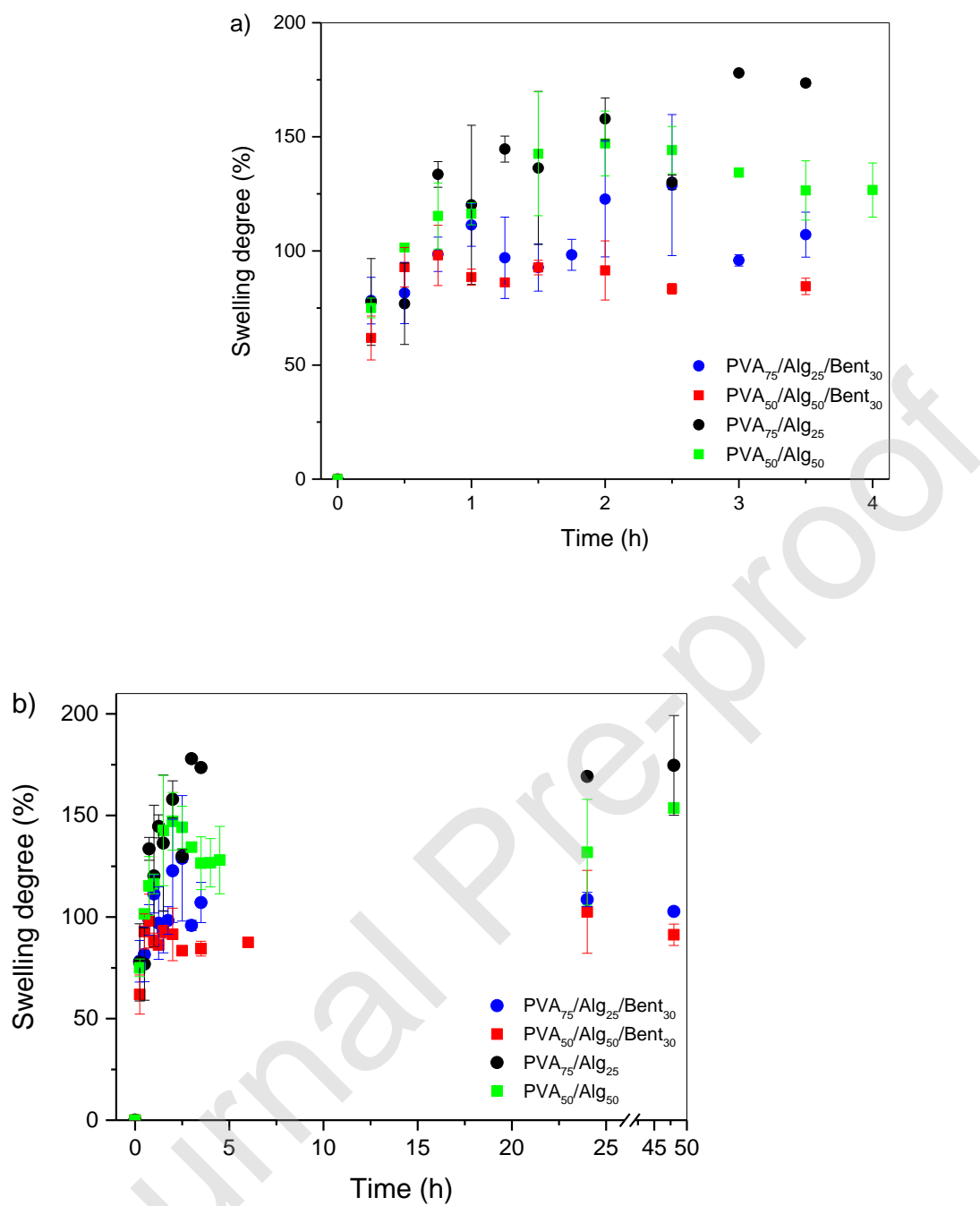


Figure 4. Swelling degree of the hydrogel beads as a function of time: a) at short swelling time; b) until equilibrium.

3.3. Qualitative chemical composition

FTIR spectra of the prepared composites beads are plotted in **Figure 5**. The different typical bands of pure compounds that have already been reported in the literature can be identified in all the spectra (Dutra et al., 2017; Gonzalez, J. S., Ponce, A., Alvarez, 2016; Hua et al., 2010; Mahdavinia et al., 2016). In the region of 3300-3400 cm^{-1} the bands of stretching of $-\text{OH}$ of the PVA and Alg overlap; in the area of 1600 cm^{-1} and 1400 cm^{-1} the bands due to asymmetric and symmetrical stretches of the $-\text{COO}^-$ of the Alg respectively can be found and at around 1000 cm^{-1} there is an overlap of the stretching of $-\text{CO}$ of PVA, the C-O-C bond of Alg and the Si-O bond of Bent. This last peak is markedly increased in compounds containing Bent which proves that the clay is incorporated in the polymer matrix. In addition, as expected, in the compounds that have a higher content of Alg, larger peaks are evident in the areas of 1400 and 1600 cm^{-1} . Small shifts are evident in the position of the peak near 1300 cm^{-1} which would be related to the presence of hydrogen bonds between $-\text{OH}$ groups of PVA and Alg or with Si-O groups of Bent (Gonzalez, J. S., Ponce, A., Alvarez, 2016; Thayumanavan, N., Tambe, P., Joshi, 2015).

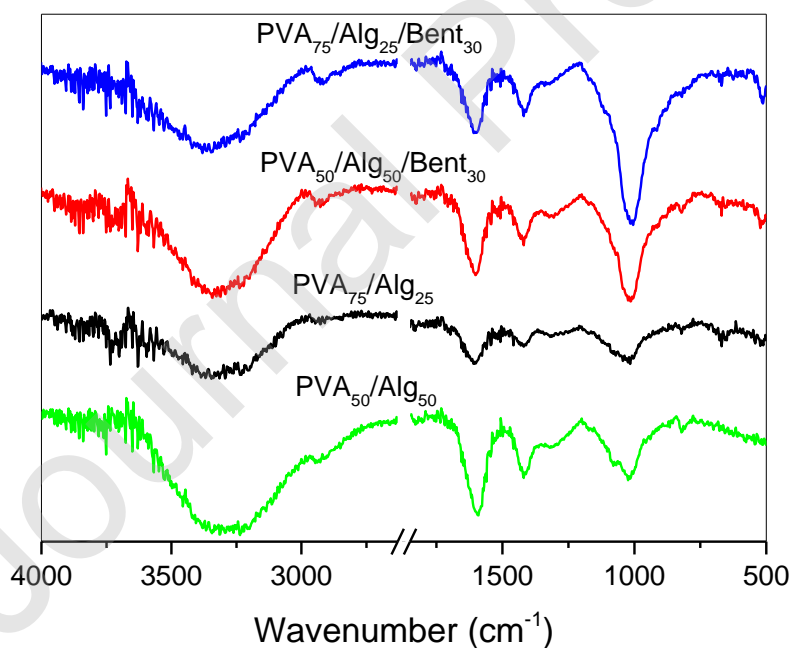


Figure 5. FTIR measurements of the prepared beads.

3.5. Arsenic removal tests

The aqueous pollutant removal results are shown in **Figure 6**. The most outstanding result that can be first mentioned is that the clay inclusion plays a key role in the As adsorption since, as can be seen, the two unfilled PVA/Alg beads were not capable to remove it. Then, although the PVA₅₀/Alg₅₀/Bent₃₀ beads achieved a higher As removal than PVA₇₅/Alg₂₅/Bent₃₀ beads at treatment times about 6 h or minor ones, when considering larger treatments times the As removal finally achieved has no significant difference.

Normally there are three stages during the adsorption processes in porous media (Zeng et al., 2019), in the case of samples PVA₅₀/Alg₅₀/Bent₃₀ and PVA₇₅/Alg₂₅/Bent₃₀ a similar result was obtained. In the first two hours, the first stage occurs where the adsorbate diffuses towards the adsorbent surface. This stage was very fast, due to the large number of adsorption sites that the porous beads have on the surface and because the concentration differences are large. In a second stage, in the 2-12 h contact time range, it is presumed that the diffusion into the beads occurs; this stage is slower than the first one due to the diffusion impediments imposed by the porous structure and the concentration difference that is decreasing. Finally, in the third stage of 12-48 h of contact time, the adsorption process reaches equilibrium and the speed remains constant. In the first stages, the removal efficiency of PVA₅₀/Alg₅₀/Bent₃₀ is better than PVA₇₅/Alg₂₅/Bent₃₀. As mentioned before, possibly, the increase of Alg proportion produces a decrease in the capacity of the PVA molecules to form hydrogen bonds (Dutra et al., 2017). This generates a lower degree of crosslinking in the PVA₅₀/Alg₅₀/Bent₃₀ system, which leads to the first stages being faster since in a more amorphous medium the diffusion is faster.

It is important to remark that the remaining As concentration after the applied treatments was found within the range recommended by the World Health Organization (WHO, 0.01-0.02 ppm) (Guo et al., 2015). Regarding the lower or null aqueous pollutant removal efficiency presented by an unfilled neat hydrogel when it is compared to the activity of its corresponding filled hydrogel, similar results were previously reported by the authors (Laura M. Sanchez et al., 2019).

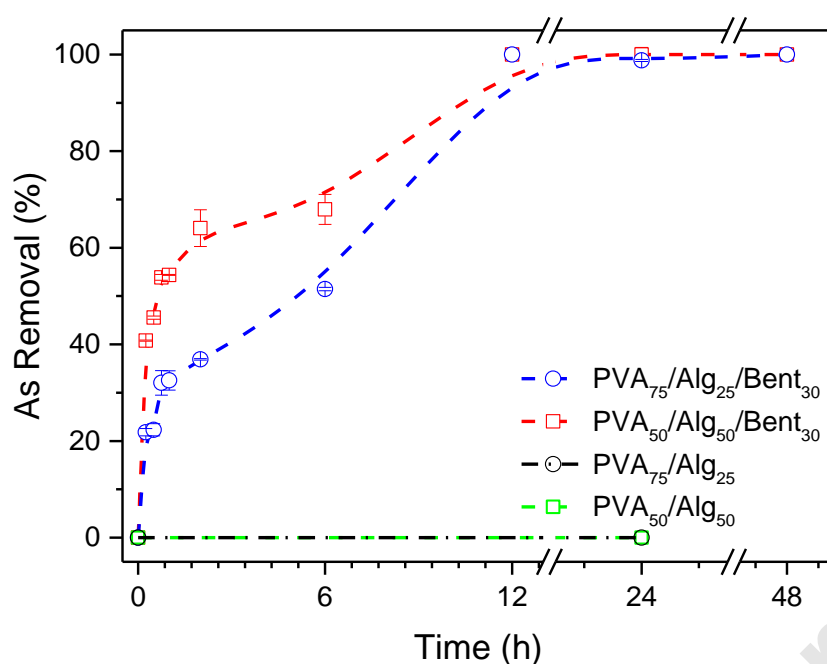


Figure 6. Arsenic removal percentages achieved by the prepared beads as a function of time.

In order to identify possible changes in the beads after their use in the removal of Arsenic from water, the FTIR spectra of the fresh beads and after 48 hours of use in water remediation are compared (**Figure 7**). Again, the same peaks that were previously discussed in Figure 6 are identified. According to the literature, the bands assigned to the different Arsenic bonds are between 800 and 900 cm^{-1} (Myneni et al., 1998) and unfortunately in our systems these peaks are overlap with those that are typical for PVA, Alg and Bent as discussed above, which does not allow us to identify the presence of As within the spheres. It is noticeable that some important changes in the spectra of the samples used for 48 hours are evident, after that time of treatment the majority of the spectrum bands are diminished, which would mean the migration of the components of the beads. This effect becomes more noticeable in the regions of 3400 cm^{-1} (-OH of PVA and Alg) and 2900 cm^{-1} (-CH- bond of PVA) and not so much in the peaks belonging exclusively to the Alg, which would indicate a greater migration of the PVA.

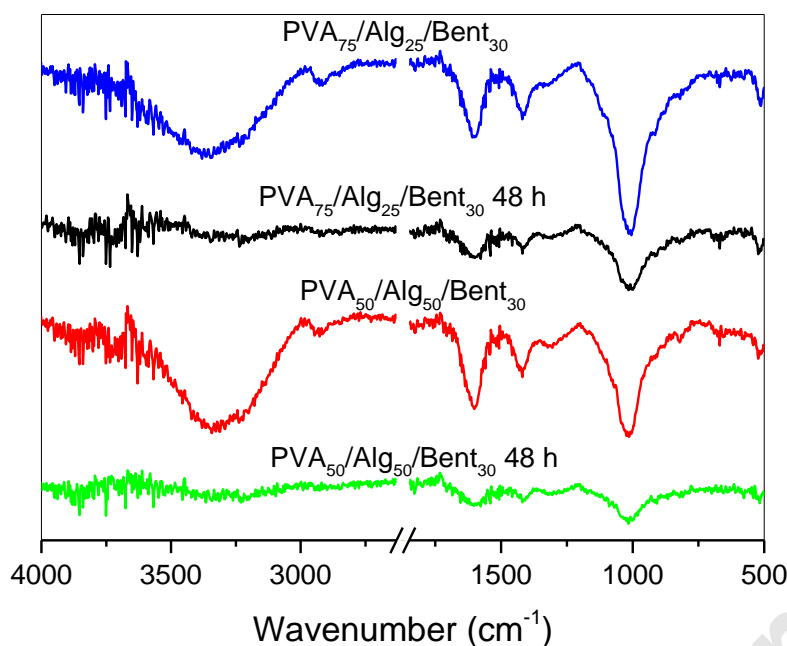


Figure 7. FTIR measurements of the composite beads before and after 48 h of water treatments.

4. Conclusions

Polyvinyl alcohol (PVA) and alginate (Alg) eco-friendly hydrogel beads with different PVA / Alg proportions containing natural bentonite were developed by external ionic gelation, characterized and evaluated as potential useful devices for As removal from polluted water. SEM micrographs of the lyophilized beads evidenced a rather compact surface and a highly porous and robust internal structure. Bentonite was uniformly dispersed and no macroscopic aggregates were observed. Besides, on the basis of the obtained results, it can be inferred that PVA was in amorphous state inside the beads. In addition, it was found that higher PVA contents are related with higher swelling degree values whereas the incorporation of clay to the hydrogels produced a reduction on the swelling degree and an increase of GF.

The results herein presented indicate that the clay inclusion plays a key role in the As removal performance of the beads. Although at short treatment times (less than 6 h), the beads containing

Bent and a higher Alg proportion evidenced a better removal efficiency, whereas at longer treatment times both Bent-containing formulations displayed complete As removal. However, the FTIR spectra of beads after As removal showed that PVA was partially extracted which can be associated with the low crosslinking and almost amorphous state within the matrix. Therefore, PVA₅₀/Alg₅₀/Bent₃₀ beads are the best sample for the proposed application. To sum up, the developed composite materials could be potentially used for As removal combining the ability of bentonite to remove As with the easy manipulation given by the polymeric beads.

CRediT authorship contribution statement

Estefanía Baigorria: Conceptualization, Methodology, Validation, Investigation, Writing - original draft, Writing - review & editing, Supervision.

Leonardo A. Cano: Conceptualization, Methodology, Validation, Investigation, Writing - original draft, Writing - review & editing, Supervision.

Laura M. Sanchez: Conceptualization, Methodology, Validation, Investigation, Writing - original draft, Writing - review & editing, Supervision, Project administration.

Vera A. Alvarez: Conceptualization, Writing - original draft, Writing - review & editing, Supervision, Resources, Project administration, Funding acquisition.

Romina P. Ollier: Conceptualization, Methodology, Validation, Investigation, Writing - original draft, Writing - review & editing, Supervision, Resources, Project administration, Funding acquisition.

Declaration of interests

The authors declare that they have no known competing financial interests or personal relationships that could have appeared to influence the work reported in this paper.

Acknowledgments

Financial support of CONICET, Universidad Nacional de Mar del Plata and ANPCyT is acknowledged.

References

- Al-Bastaki, N., 2004. Removal of methyl orange dye and Na₂SO₄ salt from synthetic waste water using reverse osmosis. *Chem. Eng. Process. Process Intensif.* 43, 1561–1567. <https://doi.org/10.1016/J.CEP.2004.03.001>
- Bera, R., Dey, A., Chakrabarty, D., 2015. Synthesis, Characterization, and Drug Release Study of Acrylamide-Co-Itaconic Acid Based Smart Hydrogel. *Polym. Eng. Sci.* 55, 113–122.
- Çaykara, T., Demirci, S., 2006. Preparation and Characterization of Blend Films of Poly(Vinyl Alcohol) and Sodium Alginate. *J. Macromol. Sci. Part A* 43, 1113–1121. <https://doi.org/10.1080/10601320600740389>
- D'Amico, D.A., Ollier, R.P., Alvarez, V.A., Schroeder, W.F., Cyras, V.P., 2014. Modification of bentonite by combination of reactions of acid-activation, silylation and ionic exchange. *Appl. Clay Sci.* 99, 254–260. <https://doi.org/10.1016/j.clay.2014.07.002>
- Dinu, M.V., Lazar, M.M., Dragan, E.S., 2017. Dual ionic cross-linked alginate/clinoptilolite composite microbeads with improved stability and enhanced sorption properties for methylene blue. *React. Funct. Polym.* 116, 31–40. <https://doi.org/10.1016/j.reactfunctpolym.2017.05.001>
- Dinu, M.V., Přádný, M., Drăgan, E.S., Michálek, J., 2013. Ice-templated hydrogels based on chitosan with tailored porous morphology. *Carbohydr. Polym.* 94, 170–178. <https://doi.org/10.1016/J.CARBPOL.2013.01.084>
- Dopp, E., von Recklinghausen, U., Diaz-Bone, R., Hirner, A.V., Rettenmeier, A.W., 2010. Cellular uptake, subcellular distribution and toxicity of arsenic compounds in methylating and non-methylating cells. *Environ. Res.* 110, 435–442. <https://doi.org/10.1016/J.ENVRES.2009.08.012>
- Dutra, J.A.P., Carvalho, S.G., Zampirolli, A.C.D., Daltoé, R.D., Teixeira, R.M., Careta, F.P., Cotrim, M.A.P., Oréfice, R.L., Villanova, J.C.O., 2017. Papain wound dressings obtained

- from poly(vinyl alcohol)/calcium alginate blends as new pharmaceutical dosage form: Preparation and preliminary evaluation. *Eur. J. Pharm. Biopharm.* 113, 11–23. <https://doi.org/10.1016/J.EJPB.2016.12.001>
- García-Carvajal, C., Villarroel-Rocha, J., Curvale, D., Barroso-Quiroga, M. M., Sapag, K., 2019. Arsenic (V) removal from aqueous solutions using natural clay ceramic monoliths. *Chem. Eng. Commun.* 206, 1451–1462. <https://doi.org/10.1080/00986445.2018.1564910>
- Ghasemzadeh, H., Ghanaat, F., 2014. Antimicrobial alginate/PVA silver nanocomposite hydrogel, synthesis and characterization. *J. Polym. Res.* 21, 355. <https://doi.org/10.1007/s10965-014-0355-1>
- Ghorbanzadeh, N., Jung, W., Halajnia, A., Lakzian, A., Kabra, A.N., Jeon, B.-H., 2015. Removal of arsenate and arsenite from aqueous solution by adsorption on clay minerals. *Geosystem Eng.* 18, 302–311. <https://doi.org/10.1080/12269328.2015.1062436>
- Goldberg, S., 2002. Competitive Adsorption of Arsenate and Arsenite on Oxides and Clay Minerals. *Soil Sci. Soc. Am. J.* 66, 413–421. <https://doi.org/https://doi.org/10.2136/sssaj2002.4130>
- Golob, V., Vinder, A., Simonič, M., 2005. Efficiency of the coagulation/flocculation method for the treatment of dyebath effluents. *Dye. Pigment.* 67, 93–97. <https://doi.org/10.1016/J.DYEPIG.2004.11.003>
- Gonzalez, J. S., Ponce, A., Alvarez, V.A., 2016. Preparation and characterization of poly (vinylalcohol) / bentonite hydrogels for potential wound dressings. *Adv Mater Lett* 7, 979–985.
- Guan, X., Du, J., Meng, X., Sun, Y., Sun, B., Hu, Q., 2012. Application of titanium dioxide in arsenic removal from water: A review. *J. Hazard. Mater.* 215–216, 1–16. <https://doi.org/10.1016/J.JHAZMAT.2012.02.069>
- Guo, L., Ye, P., Wang, J., Fu, F., Wu, Z., 2015. Three-dimensional Fe₃O₄-graphene macroscopic

- composites for arsenic and arsenate removal. *J. Hazard. Mater.* 298, 28–35.
<https://doi.org/10.1016/J.JHAZMAT.2015.05.011>
- Halter, W.E., Pfeifer, H.-R., 2001. Arsenic(V) adsorption onto α -Al₂O₃ between 25 and 70°C. *Appl. Geochemistry* 16, 793–802. [https://doi.org/https://doi.org/10.1016/S0883-2927\(00\)00066-4](https://doi.org/https://doi.org/10.1016/S0883-2927(00)00066-4)
- Hassan, C.M., Peppas, N.A., 2000. Structure and Morphology of Freeze/Thawed PVA Hydrogels. *Macromolecules* 33, 2472–2479. <https://doi.org/10.1021/ma9907587>
- Hua, J., 2015. Synthesis and characterization of bentonite based inorgano-organo-composites and their performances for removing arsenic from water. *Appl. Clay Sci.* 114, 239–246.
<https://doi.org/10.1016/j.clay.2015.06.005>
- Hua, S., Ma, H., Li, X., Yang, H., Wang, A., 2010. pH-sensitive sodium alginate/poly(vinyl alcohol) hydrogel beads prepared by combined Ca²⁺ crosslinking and freeze-thawing cycles for controlled release of diclofenac sodium. *Int. J. Biol. Macromol.* 46, 517–523.
<https://doi.org/10.1016/J.IJBIOMAC.2010.03.004>
- Inoue, S.K., 1997. A moving boundary model of calcium alginate gel formation and the estimation of diffusion and mass transfer coefficients.
- Khan, M., Lo, I.M.C., 2016. A holistic review of hydrogel applications in the adsorptive removal of aqueous pollutants: Recent progress, challenges, and perspectives. *Water Res.* 106, 259–271. <https://doi.org/10.1016/J.WATRES.2016.10.008>
- Khurana, I., Saxena, A., Bharti, Khurana, J.M., Rai, P.K., 2017. Removal of Dyes Using Graphene-Based Composites: a Review. *Water, Air, Soil Pollut.* 228, 180.
<https://doi.org/10.1007/s11270-017-3361-1>
- Kim, H.S., 1990. A kinetic study on calcium alginate bead formation. *Korean J. Chem. Eng.* 7, 1–6. <https://doi.org/10.1007/BF02697334>
- Kokabi, M., Sirousazar, M., Hassan, Z.M., 2007. PVA–clay nanocomposite hydrogels for wound

- dressings. *Eur. Polym. J.* 43, 773–781. <https://doi.org/10.1016/J.EURPOLYMJ.2006.11.030>
- Kushwaha, S.K., Saxena, P., Rai, A., 2012. Stimuli sensitive hydrogels for ophthalmic drug delivery: A review. *Int. J. Pharm. Investig.* 2, 54–60. <https://doi.org/10.4103/2230-973X.100036>
- Lenoble, V., Deluchat, V., Serpaud, B., Bollinger, J.C., 2003. Arsenite oxidation and arsenate determination by the molybdene blue method. *Talanta* 61, 267–276. [https://doi.org/10.1016/S0039-9140\(03\)00274-1](https://doi.org/10.1016/S0039-9140(03)00274-1)
- Lodha, B., Chaudhari, S., 2007. Optimization of Fenton-biological treatment scheme for the treatment of aqueous dye solutions. *J. Hazard. Mater.* 148, 459–466. <https://doi.org/10.1016/J.JHAZMAT.2007.02.061>
- Lozinsky, V.I., Plieva, F.M., 1998. Poly(vinyl alcohol) cryogels employed as matrices for cell immobilization. 3. Overview of recent research and developments. *Enzyme Microb. Technol.* 23, 227–242. [https://doi.org/10.1016/S0141-0229\(98\)00036-2](https://doi.org/10.1016/S0141-0229(98)00036-2)
- Lupo, B., Maestro, A., Gutiérrez, J.M., González, C., 2015. Characterization of alginate beads with encapsulated cocoa extract to prepare functional food: Comparison of two gelation mechanisms. *Food Hydrocoll.* 49, 25–34. <https://doi.org/10.1016/j.foodhyd.2015.02.023>
- Mahdavinia, G.R., Mousanezhad, S., Hosseinzadeh, H., Darvishi, F., Sabzi, M., 2016. Magnetic hydrogel beads based on PVA/sodium alginate/laponite RD and studying their BSA adsorption. *Carbohydr. Polym.* 147, 379–391. <https://doi.org/10.1016/J.CARBPOL.2016.04.024>
- Mahdavinia, G.R., Soleymani, M., Etemadi, H., Sabzi, M., Atlasi, Z., 2018. Model protein BSA adsorption onto novel magnetic chitosan/PVA/laponite RD hydrogel nanocomposite beads. *Int. J. Biol. Macromol.* 107, 719–729. <https://doi.org/10.1016/J.IJBIOMAC.2017.09.042>
- Masteiková, R., Chalupová, Z., Sklupalová, Z., 2013. Stimuli-sensitive hydrogels in controlled and sustained drug delivery. *Med. (B. Aires)* 39, 19–24.

- Mohapatra, D., Mishra, D., Chaudhury, G.R., Das, R.P., 2007. Arsenic adsorption mechanism on clay minerals and its dependence on temperature. *Korean J. Chem. Eng.* 24, 426–430.
<https://doi.org/10.1007/s11814-007-0073-z>
- Myneni, S.C., Traina, S.J., Waychunas, G.A., Logan, T.J., 1998. Experimental and theoretical vibrational spectroscopic evaluation of arsenate coordination in aqueous solutions, solids, and at mineral-water interfaces. *Geochim. Cosmochim. Acta* 62, 3285–3300.
[https://doi.org/10.1016/S0016-7037\(98\)00222-1](https://doi.org/10.1016/S0016-7037(98)00222-1)
- Ollier, R. P., Sanchez, L. M., Gonzalez, J. S., Alvarez, V.A., 2018. Thermal properties of hydrogel-clay nano-composites. *Adv. Mater. Lett.* 9, 505–509.
- Ozay, O., Ekici, S., Baran, Y., Aktas, N., Sahiner, N., 2009. Removal of toxic metal ions with magnetic hydrogels. *Water Res.* 43, 4403–4411.
<https://doi.org/10.1016/J.WATRES.2009.06.058>
- Paques, J.P., van der Linden, E., van Rijn, C.J.M., Sagis, L.M.C., 2014. Preparation methods of alginate nanoparticles. *Adv. Colloid Interface Sci.* 209, 163–171.
<https://doi.org/10.1016/J.CIS.2014.03.009>
- Pathan, S., Bose, S., 2018. Arsenic Removal Using “Green” Renewable Feedstock-Based Hydrogels: Current and Future Perspectives. *ACS Omega* 3, 5910–5917.
<https://doi.org/10.1021/acsomega.8b00236>
- Paulino, A.T., Belfiore, L.A., Kubota, L.T., Muniz, E.C., Almeida, V.C., Tambourgi, E.B., 2011. Effect of magnetite on the adsorption behavior of Pb(II), Cd(II), and Cu(II) in chitosan-based hydrogels. *Desalination* 275, 187–196.
<https://doi.org/10.1016/J.DESAL.2011.02.056>
- Peppas, N. A., Hansen, P.J., 1982. Crystallization Kinetics of Poly (vinyl Alcohol). *J. Appl. Polym. Sci.* 27, 4787–4797.
- Peppas, N.A., Tennenhouse, D., 2004. Semicrystalline poly(vinyl alcohol) films and their blends

- with poly(acrylic acid) and poly(ethylene glycol) for drug delivery applications. *J. Drug Deliv. Sci. Technol.* 14, 291–297. [https://doi.org/10.1016/S1773-2247\(04\)50050-3](https://doi.org/10.1016/S1773-2247(04)50050-3)
- Peralta Ramos, M.L., González, J.A., Albornoz, S.G., Pérez, C.J., Villanueva, M.E., Giorgieri, S.A., Copello, G.J., 2016. Chitin hydrogel reinforced with TiO₂ nanoparticles as an arsenic sorbent. *Chem. Eng. J.* 285, 581–587. <https://doi.org/10.1016/J.CEJ.2015.10.035>
- Perez, J.J., Villanueva, M.E., Sánchez, L., Ollier, R., Alvarez, V., Copello, G.J., 2020. Low cost and regenerable composites based on chitin/bentonite for the adsorption potential emerging pollutants. *Appl. Clay Sci.* 194, 105703. <https://doi.org/https://doi.org/10.1016/j.clay.2020.105703>
- Qiu, Y., Park, K., 2001. Environment-sensitive hydrogels for drug delivery. *Adv. Drug Deliv. Rev.* 53, 321–339. [https://doi.org/10.1016/S0169-409X\(01\)00203-4](https://doi.org/10.1016/S0169-409X(01)00203-4)
- Rahim, M., Mas Haris, M.R.H., 2015. Application of biopolymer composites in arsenic removal from aqueous medium: A review. *J. Radiat. Res. Appl. Sci.* 8, 255–263. <https://doi.org/10.1016/j.jrras.2015.03.001>
- Rajmohan, D., Bellmer, D., 2019. Characterization of spirulina-alginate beads formed using ionic gelation. *Int. J. Food Sci.* 2019. <https://doi.org/10.1155/2019/7101279>
- Ramteke, K., n.d. Stimuli Sensitive Hydrogels in Drug Delivery Systems. *Int. J. Pharm. Sci. Res.* 2012, 4604–4616.
- Ratna, D., Padhi, B.S., 2012. Pollution due to synthetic dyes toxicity & carcinogenicity studies and remediation. *Int. J. Environ. Sci.* 3, 940–955.
- Robinson, T., McMullan, G., Marchant, R., Nigam, P., 2001. Remediation of dyes in textile effluent: a critical review on current treatment technologies with a proposed alternative. *Bioresour. Technol.* 77, 247–255. [https://doi.org/10.1016/S0960-8524\(00\)00080-8](https://doi.org/10.1016/S0960-8524(00)00080-8)
- Safi, S.R., Senmoto, K., Gotoh, T., Iizawa, T., Nakai, S., 2019. The effect of γ -FeOOH on enhancing arsenic adsorption from groundwater with DMAPAAQ + FeOOH gel composite.

Sci. Rep. 9, 11909. <https://doi.org/10.1038/s41598-019-48233-x>

- Sahiner, N., Ozay, O., Aktas, N., Blake, D.A., John, V.T., 2011. Arsenic (V) removal with modifiable bulk and nano p(4-vinylpyridine)-based hydrogels: The effect of hydrogel sizes and quarternization agents. *Desalination* 279, 344–352. <https://doi.org/10.1016/J.DESAL.2011.06.028>
- Sanchez, L. M., Alvarez, V.A., 2019. Development of potentially biocompatible hydrogels with cylindrical pores prepared from polyvinyl alcohol and low-molecular weight polyacrylic acid. *Polym. Eng. Sci.* 59, 1479–1488.
- Sanchez, L. M., Ollier, R. P., Gonzalez, J. S., Alvarez, V.A., 2018. Nanocomposite Materials for Dyes Removal, in: *Handbook of Nanomaterials for Industrial Applications*. pp. 921–951.
- Sanchez, Laura M., Alvarez, V.A., Ollier, R.P., 2019. Acid-treated Bentonite as filler in the development of novel composite PVA hydrogels. *J. Appl. Polym. Sci.* 136, 1–10. <https://doi.org/10.1002/app.47663>
- Sanchez, Laura M, Ollier, R.P., Alvarez, V.A., 2019. Sorption behavior of polyvinyl alcohol/bentonite hydrogels for dyes removal. *J. Polym. Res.* 26, 142. <https://doi.org/10.1007/s10965-019-1807-4>
- Sanchez, L.M., Shuttleworth, P.S., Waiman, C., Zanini, G., Alvarez, V.A., Ollier, R.P., 2020. Physically-crosslinked polyvinyl alcohol composite hydrogels containing clays, carbonaceous materials and magnetic nanoparticles as fillers. *J. Environ. Chem. Eng.* 8, 103795. <https://doi.org/10.1016/J.JECE.2020.103795>
- Santagapita, P.R., Mazzobre, M.F., Buera, M. del P., 2012. Invertase stability in alginate beads: Effect of trehalose and chitosan inclusion and of drying methods. *Food Res. Int.* 47, 321–330. <https://doi.org/10.1016/J.FOODRES.2011.07.042>
- Sinha Ray, S., Okamoto, M., 2003. Polymer/layered silicate nanocomposites: a review from preparation to processing. *Prog. Polym. Sci.* 28, 1539–1641.

<https://doi.org/10.1016/J.PROGPOLYMSCI.2003.08.002>

Slokar, Y.M., Majcen Le Marechal, A., 1998. Methods of decoloration of textile wastewaters.

Dye. Pigment. 37, 335–356. [https://doi.org/10.1016/S0143-7208\(97\)00075-2](https://doi.org/10.1016/S0143-7208(97)00075-2)

Soares, J.P., Santos, J.E., Chierice, G.O., Cavaleiro, E.T.G., 2004. Thermal behavior of alginic acid and its sodium salt. *Eclética Química* 29, 57–64. <https://doi.org/10.1590/S0100-46702004000200009>

Sun, Y., Zhang, Z., Moon, K. S., Wong, C.P., 2004. Glass transition and relaxation behavior of epoxy nanocomposites. *Polym. Sci. Part B Polym. Phys.* 42, 3849–3858.

Tajuddin Sikder, M., Tanaka, S., Saito, T., Kurasaki, M., 2014. Application of zerovalent iron impregnated chitosan-carboxymethyl- β -cyclodextrin composite beads as arsenic sorbent. *J. Environ. Chem. Eng.* 2, 370–376. <https://doi.org/10.1016/J.JECE.2014.01.009>

Thayumanavan, N., Tambe, P., Joshi, G., 2015. Effect of surfactant and sodium alginate modification of graphene on the mechanical and thermal properties of polyvinyl alcohol (PVA) nanocomposites. *Cellul. Chem. Technol.* 49, 80.

Thomas, D.J., Styblo, M., Lin, S., 2001. The Cellular Metabolism and Systemic Toxicity of Arsenic. *Toxicol. Appl. Pharmacol.* 176, 127–144. <https://doi.org/10.1006/TAAP.2001.9258>

Tong, D., Fang, K., Yang, H., Wang, J., Zhou, C., Yu, W., 2019. Efficient removal of copper ions using a hydrogel bead triggered by the cationic hectorite clay and anionic sodium alginate. *Environ. Sci. Pollut. Res.* 26, 16482–16492. <https://doi.org/10.1007/s11356-019-04895-8>

Zeng, H., Qiao, T., Zhao, Y., Yu, Y., Zhang, J., Li, D., 2019. Characterization and Arsenic Adsorption Behaviors of Water Treatment Residuals from Waterworks for Iron and Manganese Removal. *Int. J. Environ. Res. Public Health* 16, 4912. <https://doi.org/10.3390/ijerph16244912>

Figure 1. SEM micrographs of the beads.

Figure 2. TGA and DTGA thermograms of the samples.

Figure 3. DSC thermograms of the samples.

Figure 4. Swelling degree of the hydrogel beads as a function of time: a) at short swelling time; b) until equilibrium.

Figure 5. FTIR measurements of the prepared beads.

Figure 6. Arsenic removal percentages achieved by the prepared beads as a function of time.

Figure 7. FTIR measurements of the composite beads before and after 48 h of water treatments.